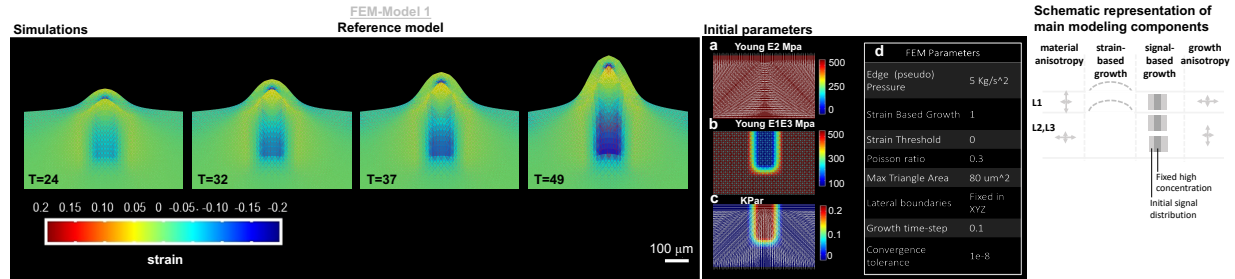
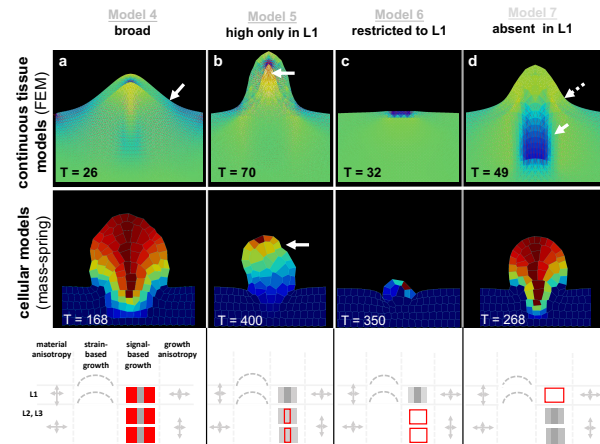


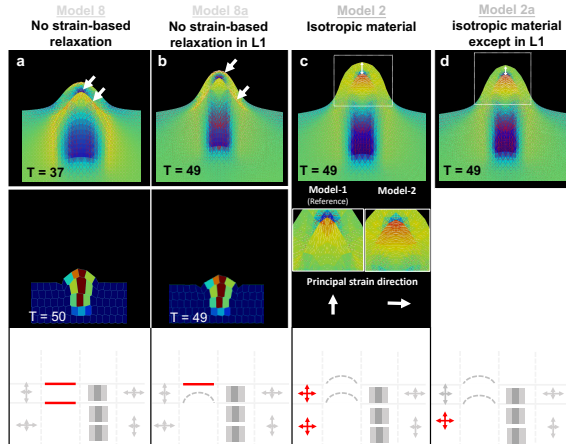
A FEM reference model



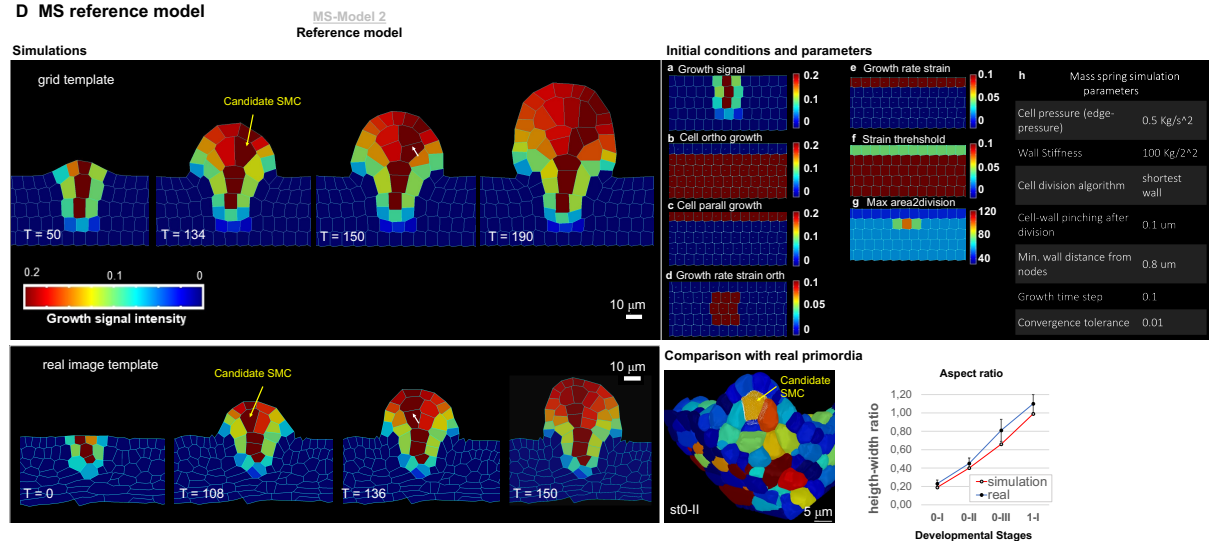
B Models varying the domain of the growth signal



C Models varying strain-based relaxation and material property



D MS reference model



E SMC division prevented at T=110

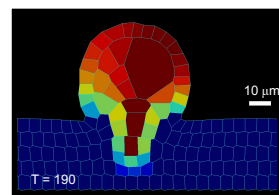


Figure 3 – figure supplement 1. Related to Figure 3. FEM- and MS-based simulations, reference models, and additional variations.

Figure 3 – figure supplement 1. Related to Figure 3. FEM- and MS-based simulations, reference models, and additional variations.

(A) *Time series of the FEM reference simulation: FEM-Model 1 and its preparation.* **Left:** reference simulation progression; the lines represent the in-plane principal strains: white for extensive, red for compressive. The heatmap represents the trace of the Green-Lagrange strain tensor. **Tables (middle):** preparation of the reference template (a-c) and initial parameters (d). (a-c) the starting template is a flat tissue representation distinguishing L1 and inner layers on which anisotropic material (a, Young's modulus E_2), material stiffness (b, Young's modulus E_1E_3), and the growth signal (c, K_{par}) domain are set. The white lines **in the images left** indicate the direction of fiber reinforcement for the anisotropic material (a), the intensity of the stiffness in the isotropic component of the material (b), the direction of signal-based growth, which is orthogonal to the fiber reinforcement direction (c). In addition, all lateral boundaries of the simulation template (except the top one) were fixed in all degrees of freedom. The table (d) integrates the visual information with global parameters. See additional explanations in the [STAR Methods](#). **Schematic representation (right) of the main parameters modulated in the models shown in B and compared to the reference model for the L1 and underlying (L2,L3) layers.** Arrows of different size indicate anisotropy, the bulged dotted line represent the ability of the tissue to (passively) grow under strain, the grey fields represent the initial domain distribution of the growth signal (pale grey) and the domain of fixed, high concentration (dark grey square). Deviations of these parameters are shown in red in the panel B.

(B) *Variation of the signal-based growth distribution with respect to the FEM- and MS-based reference models.* For all model variations, the result is shown for the continuous FEM-based simulations (**top**) and the MS-based simulations (**middle**) at the simulation time point indicated (T), **a schematic representation of the altered parameter is shown in red following the scheme template in A (bottom).** color scale: same as in panel A and D for FEM- and MS-models, respectively. **(a)** Model 4: the signal is allowed to diffuse broadly. In both FEM- and MS-based simulations, the primordium is broader and the flanks are not orthogonal to the surface (arrow) as in the reference models. **(b)** Models 5: L1-driven growth hypothesis (1). Here the growth-specifying signal is set at a high and fixed (i.e., non-diffusing) concentration only in the L1. In both simulations, these conditions allow the formation of a protrusion but not a realistic primordium. For both simulations, the growth time went beyond the reference time to reach the same final height as in the reference models and to compensate for the prescribed reduced growth intensity. Specific observations are made for the different simulations: FEM-Model 5 shows high compression forces below the L1 (arrow: compressive areas are marked by the blue color and red lines). One interpretation is that these compressions may arise because the L1 “collapses” towards the center in the absence of inner tissue growth. Note the narrower apical, subepidermal domain than in the reference model. Furthermore, in the periclinal direction the L1 experiences significant compressions (indicated by the red lines). MS-Model 5: the growth is not balanced and generated an unstable apex (arrow, winding in different directions during growth, see [Movie S2](#)). **(c)** Models 6: L1-driven growth hypothesis (2). Here the growth signal is restricted solely to the L1. In this case, the difference is striking for both FEM- and MS-based simulations: the models are not able to create a significant buckle and, even if strain-based growth is permitted, the inner tissue is not pulled upwards. The growing part of the L1 ends being compressed by

the non-growing counterpart (as shown by the compressive strain marked in blue in the image for the FEM-based simulation), causing the simulation to numerically fail earlier than the reference (FEM) or in any case not forming a primordium (MS). **(d)** Models 7: exclusive inner-tissue growth hypothesis. Here, the growth signal is absent in the L1. The L1 performs exclusively passive strain-based relaxation. In this model, we test whether it is plausible that growth can be entirely initiated by the inner tissues, provided the L1 has a higher ability to relax (compared to the remaining tissue) due to induced strain. In such a scenario, the inner layer, which is prescribed to grow as in the reference model, pushes the L1, causing accumulation of tensile strains in the periclinal direction that get released due to passive strain-based relaxation. Both FEM- and MS-based simulations are able to produce a digit-shaped protrusion, even if, in the FEM-based simulation, it is shorter with less straight flanks (i.e., smoother transition from the placenta to the flanks; dotted arrow). This can be explained by the absence of compressive strains at the base of the ovule (plain arrow) in comparison with the reference model. The MS-based model displays a primordium with increased width at the apex. A possible explanation for this may be the absence of growth constraints generated by the L1. In both cases, the passive strain-based relaxation coefficient of the L1 was higher than in the reference model. Whether this is biologically relevant remains to be addressed experimentally.

(C) Models varying passive strain-based relaxation and material properties. Results are shown for the continuous FEM-based simulations (top) and the MS-based simulations (bottom) at the simulation time point indicated (T). **(a)** Models 8: absence of passive strain-based relaxation in all the tissue. In both simulations, this results in a poorly developed primordium (and numerically the simulation fail earlier than the reference time), likely due to the accumulation of high strains (and stresses), particularly visible in the FEM-based model (high accumulation of compressive and tensile strains near each other in the inner tissue as well as in the L1, arrows). **(b)** Model 8a: variation of the previous model with absence of passive strain-based relaxation only in the L1. In both simulations, the primordium is shorter than in the reference case, although less severe in the FEM-based simulation. Specifically, in the L1 there is a high accumulation of tensile stresses on the outer walls in the apical portion and in the inner walls at the base (arrows). **(c)** FEM-Model 2: absence of anisotropic material properties in all tissues. Although the simulation produced a well-shaped primordium, the L1 is slightly thicker (double sided arrow, 1.2-fold compared to reference Model 1) and there is a larger L2,L3 apical domain characterized by a principal strain oriented 90° to that in the reference model (insets). These morphological differences with the reference model can be explained by the fact that passive strain-based relaxation in an isotropic material has an equal effect in the periclinal and the anticlinal direction, producing a thicker L1 and a rounder dome. In **(d)** FEM-based Model 2b: variation of previous Model 2. Here, only the L1 has anisotropic material properties. This restores the L1 thickness control but the abnormally high intensity and modified direction of compressive strains are similar to that in Model 2.

(D) Mass spring reference model and initial template preparation, comparison with data from real ovules. Top left: MS-Model 2 simulation at four different time points. The heatmap indicates the intensity of the growth-specifying signal. Bottom left: reference simulation performed on a template obtained from a real ovule placenta (see also [STAR Methods](#)). Top right: Initial parameters at simulation start. Field values as indicated **(a-g)** used to set up the reference configuration shown on the placenta at simulation time 0 and

MS global parameters (**h**). More details can be found in the [STAR Methods](#). Bottom right: comparison between simulation and real primordia. *Image*: 3D, segmented ovule primordia stage 0-II from the wild-type reference set (see main text), longitudinal view: the SMC (orange) is outlined in a white triangular mesh (color-code refers to cell volume). Its morphology is to be compared to SMC candidates produced in the reference Model MS-Model 2 (e.g., $T=134$ for grid-based simulation and $T=108$ for real-image template-based simulation): the cell is elongated, centrally located in the apical dome and presents a broader upper periclinal wall surface compared to the bottom one. *Plot*: comparison of height-width ratio along simulation progression in MS-Model 2 and developmental progression in real (from segmented images of the wild-type reference set, see main text). For the simulation, two equi-distanced time-points between the 1st ($T = 0$) and the last simulation time step ($T = 190$) have been used to compute the values for intermediate phases.

(E) *Model intervening on SMC division*. In the reference MS-Model 2, there is no explicit rule preventing division of the SMC candidate. To analyze the consequence of SMC growth on primordium growth in our models, we prevented the SMC candidate to divide at simulation time $T = 110$. Under the reference conditions where the turgor pressure is the same among all subepidermal cells, this generates a gigantic cell exerting a considerable tensile stretch on the surrounding cells, deforming the whole domain. This suggests that, in reality, SMC growth might be compensated by a reduction in turgor pressure, a hypothesis that needs to be tested. Note that the two direct adjacent cells have an elongated shape reminiscent of companion cells.